A Low Background Magneto-Optic Probe for High Sensitivity SQUID Susceptometer

Shi Li, Daniel Hurt, Melinda Toth, Benjamin McElfresh, Andreas Amann, and Stefano Spagna

Quantum Design Inc., San Diego, CA 92121 USA

We present a magneto-optic probe designed for the studies of photoinduced magnetization in the highly sensitive SQUID susceptometer MPMS 3. The apparatus is used to conduct light from an external light source into the sealed sample chamber of the susceptometer and deliver the light stimuli right onto the sample, thus allowing uninterrupted measurement as functions of temperature and field, from 1.8 to 350 K, and in magnetic field up to 7 T. The fiber optic sample holder (FOSH) consists mostly of quartz components in order to minimize magnetic background. With background subtraction, the moment resolution of the FOSH can reach 10^{-6} emu range even at full field. Future designs are underway to further reduce the magnetic background of the sample holder.

Index Terms— **Magneto-optic (MO), photoinduced magnetization, Prussian blue, SQUID.**

I. Introduction

PHOTOINDUCED magnetization, or the manipulation of magnetic properties by light, continues to be an area of active research that attracts considerable attention [1]. Photoinduced changes in magnetic order were reported in different materials and systems, including molecule-based magnets [2], magnetic semiconductor heterostructures, [3] and manganite films [4]. In these studies, dc and ac magnetization measurements are standard techniques used to characterize light-induced magnetic changes of the sample as functions of temperature and external applied field. In this regard, modern SQUID susceptometers, such as the MPMS 3 (Quantum Design, Inc.), offers an ideal platform with high sensitivity and dynamic temperature and magnetic field control to accommodate a wide variety of samples.

The technical challenges involved are, first, to introduce light stimuli to a sealed sample with sufficient efficiency at the desired temperature or field set points so data collection is seamless and complete. Second, the apparatus for delivering the external stimuli *in situ* should contribute minimal magnetic background to the measurement.

We have developed a low background magneto-optic (MO) probe compatible with the MPMS 3 SQUID system. Alternatively called the fiber optic sample holder (FOSH, for short), it is designed to meet the above criteria for investigations of photoinduced magnetization and related effects in small solid samples. This project was motivated by experimental needs in this paper of a wide variety of MO materials, to take advantage of the 10^{-8} emu sensitivity of the SQUID susceptometer, as well as to access the full temperature range from 1.8 to 350 K, and applied magnetic field up to 7 T.

II. Hardware Design

The detection coil in the MPMS 3 system is configured as a second-order gradiometer to reduce noise caused by the fluctuations in the strong magnetic field of the superconducting magnet, and also to minimize background drifts in the SQUID detection circuit caused by the relaxation of this magnet. On the other hand, the detection coil is very sensitive to local changes in magnetic flux density. By moving a sample through the detection coil, a superconducting current is induced in the SQUID circuit and is in turn amplified and converted to an output voltage. In the standard measurement modes, sample is mounted in a sample holder that is attached to a rigid sample rod. The top of the sample rod is secured to a high precision transport motor via magnetic locks. During the measurement sequence, this whole assembly is sealed in a sample chamber under helium pressure of a few torr. In order to conduct light from an external source into the sealed sample chamber, and onto the sample in the sample holder, a special FOSH assembly consisting of FOSH sample rod, FOSH sample holder, and wired access port (WAP) is designed.

A. FOSH Sample Rod

The construction of the FOSH probe consists of several specialized hardware components as shown in Fig. 1. The foundation is the FOSH sample rod, which consists of the fiber optic bundle, and solid fiber optic rod. The fiber optic rod is fixed inside the FOSH sample rod and extends down into a special quartz sample holder. The FOSH delivers the light generated by a light source (from IR to UV range) to the quartz sample holder, which couples to the end of the sample rod. For this fiber, the attenuation of a light source of a 300 nm wavelength is ~0.4 dB for a 2 m length.

B. Wired Access Port

The light source used is a monochromatic light source (MLS) with Xenon lamp bulb, which provides the highest radiation power in UV and VIS range. A filter is used to generate light with a specific wavelength, with available filtering range between 360 and 845 nm. The typical output power at the sample for a filter with a 50 nm bandwidth is in the range of 1 to 10 mW.

Manuscript received March 6, 2014; accepted May 26, 2014. Date of current version November 18, 2014. Corresponding author: S. Li (e-mail: sli@qdusa.com).

Color versions of one or more of the figures in this paper are available online at http://ieeexplore.ieee.org.

Digital Object Identifier 10.1109/TMAG.2014.2327476

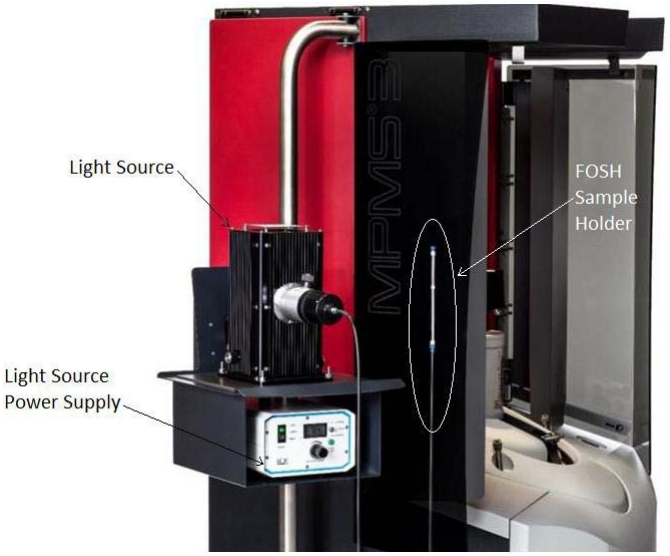

Fig. 1. MPMS 3 FOSH apparatus with MLS and power supply, FOSH sample rod, and FOSH sample holder.

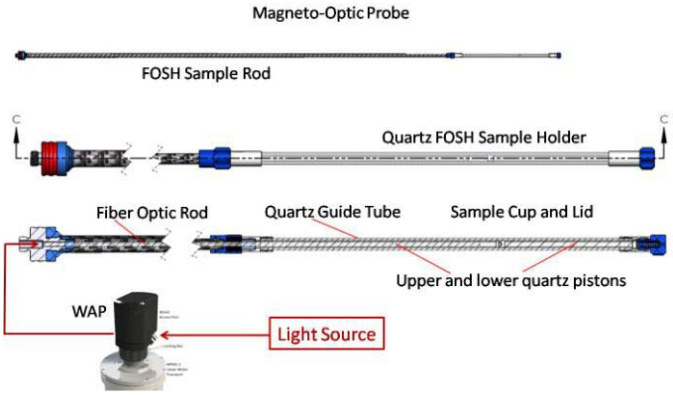

Fig. 2. Schematic diagram of the FOSH apparatus with components, including light Source, WAP, and FOSH sample rod and sample holder. Cross-sectional view of the sample holder shows its subcomponents as quartz guide tubes, sample cup and lid, and loading spring.

The WAP, with standard SMA connectors, serves as the interface for coupling fiber optic components once the sample rod has been inserted into the sample chamber, which is sealed from atmospheric pressure and filled with a few torr of helium gas.

C. FOSH Sample Holder

The sample holder (Fig. 2) is enclosed and mechanically supported by an outer quartz tube, called the guide tube. This guide tube is mounted to the bottom of the sample rod through a plastic threaded fitting. The fiber optic rod protrudes from the bottom end of the sample rod and extends approximately to the midpoint of the guide tube. The sample is mounted in a small quartz cup, with inner diameter of 1.6 mm and a depth of 1.6 mm. The sample is held in place by a quartz lid, which is held flush against the upper piston assembly by a lower piston assembly. A gentle upward pressure is maintained on all of these sliding parts by a beryllium copper spring that is mounted in a threaded cap on the bottom end of the guide tube. The arrangement ensures that the sample is securely fixed in place, and does not shift during measurements, which would otherwise induce noise in moment data.

The sample holder is designed to minimize effects that would interfere with magnetic measurements on the sample itself. The SQUID magnetometer utilizes second-order gradiometer detection coils and thus is extremely sensitive to minute non-uniformity in the sample holder over the measurement scan length [5]. The structure near the sample is made almost entirely of quartz in order to minimize the magnetic moment and magnetic noise produced by the sample holder. Since the algorithms used to determine the sample moment assume a compact, symmetrical sample, the sample holder is designed so that its magnetic properties are uniform along its full length, except for the small void represented by the sample cup. In order to maintain the symmetry between the upper and lower halves of the sample holder, the lower piston assembly is constructed from the same quartz tube and plastic-jacketed quartz fiber optic as the upper piston assembly.

III. Results

The magnetic properties of the FOSH sample holder were thoroughly investigated using both the VSM and dc scan measurement modes on the MPMS 3. We also tested a sample with MO properties using the FOSH apparatus.

A. Magnetic Background Study

We studied the magnetic background of the sample holder assembly thoroughly by measuring the components separated and assembled. The magnetic moment of the sample holder is approximately the same as that of a void in a uniform piece of quartz. Because quartz is diamagnetic, the magnetic moment of the void is proportional to magnetic field, but opposite in sign to that of a diamagnetic sample. The magnitude of the antidiamagnetic, or apparently paramagnetic, signal is on the order of 10^{-4} emu at full applied magnetic field of 7 T.

Exemplary background data for the MO sample holder is shown in Fig. 3, for the field dependence of the dc moment at 300 K. Moment versus field was measured from -7 to 7 T, with uniform spacing in field of 2000 Oe increments, and a sweep rate of 600 Oe/s. The dc scan parameters were set to measure a 30 mm (3 cm) scan length over 5 s with a total of three scans per measurement. The sample holder moment is linear with field, consistent with typical paramagnetic behavior of a void in a uniform piece of quartz. The magnitude of the background dc moment is $\sim 8.1 \times 10^{-5}$ emu at the full field of 7 T. For small moment samples, point-by-point background subtraction method can further increase the moment resolution by an order of magnitude ($\sim 1 \times 10^{-6}$ emu at full field), as indicated by the dashed blue line in Fig. 2.

B. DC Scan Versus VSM Mode

MPMS 3 is capable of seamlessly supporting two different measurement techniques, dc scan and VSM, with advances in the motion control and measurement detection circuit design.

In the dc scan mode, a sample is moved through the detection coil using a linear motion with constant speed.

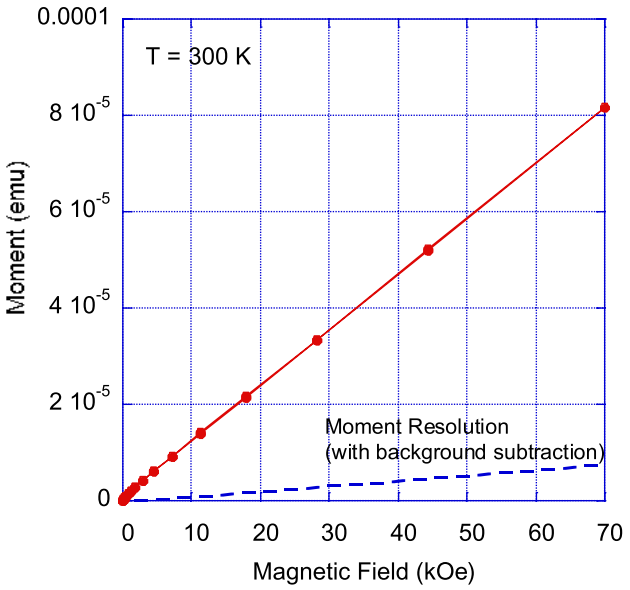

Fig. 3. Magnetic moment (dc) of FOSH sample holder (empty) as a function of applied field at 300 K. With background subtraction, the moment resolution of FOSH probe could reach 10^{-6} emu range even at full field.

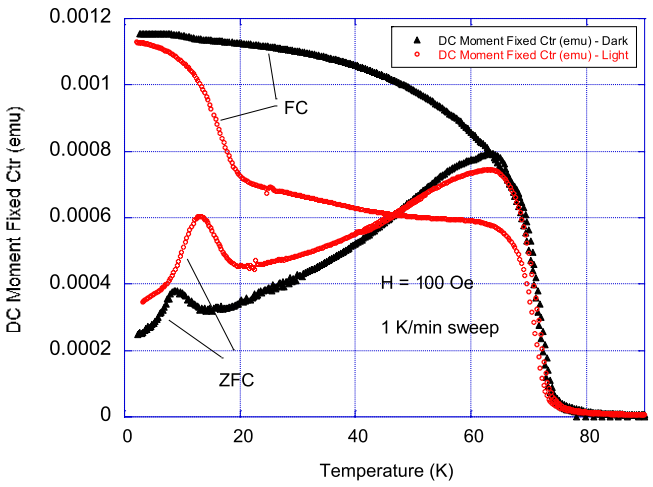

Fig. 4. ZFC–FCC magnetic moment as a function of temperature showing the large difference between the dark state (black curves) and light state (red curves) of a photoactive sample.

Fig. 5. Improved FOSH sample holder design where the bottom loading spring is moved to the top of the sample holder in order to reduce background signal thus further improve moment resolution.

The induced voltage in the SQUID detection circuit is recorded as a function of sample position, which is the raw data used in a fitting algorithm to obtain the magnetic moment of the sample. This is a big advantage of the dc scan mode, since the raw data can be saved and used later for post processing such as background subtraction when the sample signal is comparable with the background. In addition, the speed of the scan can be slowed down significantly for the FOSH probe, often necessary at very low temperatures, where the moment of the FOSH sample holder creates a heat shuttling effect in the narrow sample chamber, which could lead to temperature instability.

Since there always will be intrinsic dc drifts in the SQUID signal, which result from various sources like magnet drift, sample position movement, and so forth, we need to ensure that our analysis of the signal is not affected by them. In the dc scan mode, each measurement contains both an up scan and a down scan, and the signal due to SQUID drift is removed by subtracting these two scans before the fitting algorithm is applied. This technique has limitations though when the sample moment is small while the applied field is large.

In such cases, VSM technique has added advantage because its lock-in detection method rejects SQUID drift very effectively. In the VSM mode, the sample is vibrated around the center of the detection coil using a cosine function with frequency f, whereas lock-in detection takes place at frequency $2f$. Our five-quadrant lock-in technique removes linear drifts from VSM measurements. The $2f$ detection and the five-quadrant lock-in couple together to quickly and precisely isolate the sample signal from other noise sources, including drifts to produce a superlative VSM lock-in technique [5].

C. Sample Measurement

To test the effectiveness of the FOSH probe, we studied a photoactive compound, which consists of core shell particles of Prussian blue analogs, composed of shells of $K_{1.6}Ni_4[Cr(CN)_6]_{3.2} \cdot 4.6H_2O$ (A), which is ferromagnetic with $T_c \sim 70$ K, surrounding cores of $Rb_{0.7}Co_4[Fe(CN)_6]_{2.9} \cdot 6.6H_2O$ (B), which is photoactive and ferrimagnetic with $T_c \sim 20$ K [6].

A few milligrams of the sample were placed in the quartz sample cup then loaded into the FOSH sample holder. Center position was predetermined using a piece of nickel wire, which has a large magnetic moment relative to the FOSH holder. Temperature dependence of magnetization, the so-called zero-field-cooled (ZFC) and field-cooled (FC) curves, were measured first without illuminating the sample, which is labeled the dark state (black curves in Fig. 4). Afterward, the system temperature was stabilized at 90 K, and sample was illuminated for 2 h to activate. The light was then turned OFF, and the ZFC and FC data were collected (the light state, red curves) which shows marked moment reduction induced by light stimulation.

The dc scan method was used for the above measurement data. We also measured the sample with VSM technique,

where data quality was slightly better compared to dc scan data.

D. AC Susceptibility

Another useful option MPMS 3 can offer is the ac susceptibility measurement, which is of importance in this paper of MO materials. Because the FOSH sample holder is constructed almost entirely out of quartz material, the ac frequency scan of the empty FOSH holder shows essentially zero out-of-phase component within the entire frequency range, from 0.1 to 1000 Hz.

IV. Conclusion

In the next generation FOSH probe design, we aim to reduce the relatively high background of the sample holder. This may have been due to the metallic spring located at the bottom of the sample holder, which place a lot of background moment close to the pickup coils and to the sample. The parts at the bottom also risk rubbing on the inside of the sample chamber.

The largest design change would be to move the spring from the bottom of the FOSH sample holder to its top. This can be accomplished by a connector assembly between the FOSH sample rod and sample holder, which houses a spring that pulls the sample holder and rod together. Initial tests of the prototype shows that the magnetic background of the sample holder is reduced significantly. The new FOSH design is shown in Fig. 5, along with the improved WAP.

Acknowledgment

The authors would like to thank E. S. Knowles and M. W. Meisel at the Department of Physics, University of Florida, Gainesville, FL, USA, and National High Magnetic Field Laboratory, Tallahassee, FL, USA, for the fiber optic sample holder (FOSH) sample measurements, and C. H. Li and D. R. Talham at the Department of Chemistry, University of Florida, Gainesville, FL, USA, for sample synthesis. They would also like to thank Dr. N. Dilley for insightful discussions on FOSH background measurement.

References

[1] D. A. Pejakovic, J. L. Manson, J. S. Miller, and A. J. Epstein, "Manipulating magnets with light: Photoinduced magnetism of cobalt-iron Prussian blue analogs," *Current Appl. Phys.*, vol. 1, no. 1, pp. 15–20, 2001.

[2] J. S. Miller and A. J. Epstein, "Molecule-based magnets-an overview," *MRS Bull.*, vol. 25, no. 11, pp. 21–30, Nov. 2000.

[3] S. Koshihara *et al.*, "Ferromagnetic order induced by photogenerated carriers in magnetic III–V semiconductor heterostructures of (In, Mn) As/GaSb," *Phys. Rev. Lett.*, vol. 78, no. 24, p. 4617, 1997.

[4] J.-W. Yoo, R. S. Edelstein, D. M. Lincoln, N. P. Raju, and A. J. Epstein, "Photoinduced magnetism and random magnetic anisotropy in organic-based magnetic semiconductor V(TCNE)$_x$ films, for $x \sim 2$," *Phys. Rev. Lett.*, vol. 99, no. 15, p. 157205, 2007.

[5] D. Hurt, S. Li, and A. Amann, "Versatile SQUID susceptometer with multiple measurement modes," *IEEE Trans. Magn.*, vol. 49, no. 7, pp. 3541–3544, Jul. 2013.

[6] M. F. Dumont *et al.*, "Photoinduced magnetism in core/shell prussian blue analogue heterostructures of $K_j Nik[Cr(CN)_6]_l \cdot nH_2O$ with $Rb_a Co_b[Fe(CN)_6]_c \cdot mH_2O$," *Inorganic Chem.*, vol. 50, no. 10, pp. 4295–4300, 2011.